

Noise Due to Backscatter Off Baffles, the Nearby Wall, and Objects at the Far end of the Beam Tube; and Recommended Actions (LIGO Technical Report LIGO-T940063-00-R)

Eanna Flanagan and Kip S. Thorne

Theoretical Astrophysics, California Institute of Technology, Pasadena, CA 91125

(2 August 1994)

We have evaluated, analytically, the gravitational-wave noise in LIGO due to scattered light that backscatters off baffles far from each mirror (at distances $l \gtrsim 120$ m), off the bare vacuum tube wall near the mirror ($l \lesssim 120$ m), and off objects at the far end of the beam tube.

We find that, if there is a several-fold amplification of the baffle vibrations due to seismic noise exciting beam-tube normal modes, and if the seismic noise is *not* substantially below the LIGO specification, $10^{-7} \text{ cm Hz}^{-1/2} (f/10\text{Hz})^{-2}$, then the baffle-backscatter noise will significantly exceed the goal of 1/10 the standard quantum limit. This leads to *Recommendation 1: Serious consideration should be given to changing the baffle material from the same oxidized steel as the walls are made of, to Martin Black or some other material with a comparably low backscatter probability.* This would lower the backscatter noise by a factor $\simeq 3$.

We argue that theoretical estimates cannot be trusted to tell us how the amount of backscatter from the bare tube wall varies with the incident/backscatter angle θ_{bs} at small θ_{bs} . (Our convention is $\theta_{\text{bs}} = 0$ for grazing incidence.) If, as was assumed in the previous BRO-Weiss-Whitcomb estimates, the probability $dP/d\Omega_{\text{bs}}$ for an incident photon to backscatter into a unit solid angle is proportional to $\sin\theta_{\text{bs}}$, then we agree that backscatter off the nearby bare beam-tube wall is not a serious worry. However, if $dP/d\Omega_{\text{bs}}$ is independent of θ_{bs} , as we argue it could be, then backscatter off the bare wall will produce noise nearly identical to that from all the tube's baffles, and thus the bare-wall noise will be a serious issue. These results motivate two recommendations, which we number 2 and 4, and which we augment by a third recommendation that is important for other aspects of light-scattering noise: *Recommendation 2: The backscatter probability $dP/d\Omega_{\text{bs}}$ should be measured for the LIGO wall material at small angles, $0.005 \lesssim \theta \lesssim 0.1$. Recommendation 3: The wall material's specular reflectivity should also be measured for this same range of angles. Recommendation 4: If $dP/d\Omega_{\text{bs}}$ turns out not to fall off strongly with decreasing θ_{bs} , serious consideration should be given to baffling the nearby beamtube wall with Martin-black baffles.*

We find that, if objects at the far end of the beam tube backscatter with the same $dP/d\Omega_{\text{bs}}$ as the baffles, and if they vibrate with the same displacement spectrum, then their backscatter will produce noise ~ 2 times greater than that from the baffles; and their noise would be even larger than this if (as one measurement of a sample mirror suggests) the test-mass mirrors' scattering is enhanced over the $dP/d\Omega_{\text{ms}} = \alpha/\theta^2$ law at the tiny angles $1.5 \times 10^{-4} \gtrsim \theta \gtrsim 3 \times 10^{-5}$ of the beam tube's far end. This motivates *Recommendation 5: When instrumenting and baffling each test-mass chamber, careful attention should be paid to backscattering of light that arrives from test-mass mirrors at the far end of the beam tube.*

I. INTRODUCTION AND SUMMARY

The present configuration for the LIGO beam tube is shown in Figure 1. The test mass is ~ 10 or 30 meters from the end of a bare-walled 1.8 meter diameter tube; at the gate valve, the tube narrows to 1.2 meters and its wall remains bare for an additional 100 meters, where the first baffle is encountered. From there onward, baffles hide the tube wall from the view of the test mass. The baffles are made of the same oxidized steel as the tube.

In the analysis that follows, for simplicity we treat the tube as though it had a constant diameter of 1.2 meters, thereby making an error no larger than a few tens of percent in the noise due to bare-wall backscatter and no significant error in noise due to baffle backscatter.

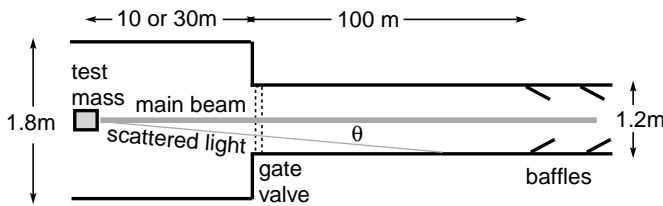


FIG. 1. Present configuration of LIGO beam tube.

Previous studies of scattered light in the LIGO beam tubes [1,2] have shown that the most serious noise source is due to baffle backscatter—i.e., due to light that is scattered, by a test-mass mirror, out of the main beam and toward a baffle, and that then backscatters off the baffle and back to the mirror, and then scatters back into the main beam (cf. Fig. 1). In this report we recompute the baffle-backscatter noise, and also noise due to backscatter from the ~ 120 meters of bare wall preceding the first baffle and from objects at the far end of the beam tube. We summarize our conclusions and recommendations in the following three subsections, and then present our computations in Sec. II and Appendices A, B and C.

A. Backscatter Off Baffles

In Sec. II we show that the gravity-wave noise produced by baffle backscatter is given by the following formula [Eq. (31)]:

$$\begin{aligned} \tilde{h}(f) &= \left[4\pi\alpha^2\beta \ln\left(\frac{l_1}{l_2}\right) J_0(\rho) \right]^{1/2} \bar{A}(f) \frac{\lambda}{R} \frac{\tilde{\xi}_s(f)}{L} \\ &= \frac{3 \times 10^{-25}}{\text{Hz}^{1/2}} \left(\frac{10\text{Hz}}{f} \right)^2 \bar{A}(f) \frac{\sqrt{J_0(\rho)}}{2} \frac{\alpha}{10^{-6}} \left(\frac{\beta}{0.01} \right)^{1/2} \\ &\quad \times \left(\frac{\ln(l_1/l_2)}{\ln(4\text{km}/120\text{m})} \right)^{1/2} \frac{\tilde{\xi}_s(f)}{10^{-7}\text{cmHz}^{-1/2}(f/10\text{Hz})^{-2}}. \end{aligned} \quad (1)$$

Here the various symbols have the following meanings: The probability for a photon in the main beam to scatter off a mirror and into a direction making an angle θ to the main beam, per unit solid angle, is assumed (in accord with previous work [1–3]) to be $dP/d\Omega_{\text{ms}} = \alpha/\theta^2$, with $\alpha \simeq 10^{-6}$. The probability for a photon arriving at a baffle from the scattering mirror to backscatter back toward that same mirror, per unit solid angle, is assumed (in accord with measurements by the Breault Research Organization, BRO [4]) to be $dP/d\Omega_{\text{bs}} = \beta \simeq 10^{-2}$; and this is true whether the photon hits the back face of a distant baffle or the front face of a more nearby baffle. The most distant baffle is at a distance $l_1 \simeq 4\text{km}$ from the mirror, and the nearest baffle is at a distance $l_2 \simeq 120\text{m}$. The mirror is offset from the center of the beam tube’s cross section by a distance ρR , where $R = 60\text{cm}$ is the beam-tube radius; and the function $J_0(\rho)$ (not a Bessel function), which deals with this offset, is plotted in Fig. 3 of Appendix C. The spectrum of the baffles’ horizontal vibrational displacement is $A(f)\tilde{\xi}_s(f)$, where $\tilde{\xi}_s(f)$ is the horizontal seismic noise spectrum and $A(f)$ accounts for amplification due to excitation of beam-tube normal modes; the quantity $\bar{A}(f)$ is an average of $A(f)$ over all regions of all baffles, with the average weighted by the backscattered light amplitude that is returned to the main beam from each region of a baffle. We choose as our fiducial seismic noise spectrum the upper-limit specification for LIGO sites in the 10 to 100 Hz band, $\tilde{\xi}_s(f) = 10^{-7}\text{cm/Hz}^{-1/2}(f/10\text{Hz})^{-2}$. Finally, $L = 4\text{km}$ and $\lambda = 0.5\mu\text{m}$ are the beam-tube length and the wavelength of the main-beam light.

Equation (1) is in fairly good agreement with Thorne’s previous estimate, Eq. (3.30) of Ref. [1] after N_b in that estimate is replaced by expression (2.5) of [1] and after the erroneous factor $1/B$ in that estimate is deleted. After these changes, the only significant remaining differences between Eq. (1) and the previous estimate are: (i) the π in Eq. (1) was a 4 in the previous estimate; (ii) the function $\sqrt{J_0(\rho)}$ was approximated in the previous estimate by $1/(1-\rho)^{3/2}$ [an approximation that overestimated the noise in the worst case, $\rho = 2/3$, by about a factor 3]; (iii) different numerical values were used for various parameters in the previous estimate.

Expression (1) has the nice feature that it is independent of most details of baffle spacing and height. As the derivation in Sec. II shows, so long as the entire beam-tube wall, from a distance l_2 to $l_1 = L$, is hidden from the scattering mirror’s view by baffles, and the baffle heights are small compared to the beam-tube radius, then other details of the baffle distribution have no significant influence on the noise. Expression (1) also shows that the noise is not very sensitive to the distance l_2 to the nearest baffle: If the nearest baffle were moved inward from $l_2 \simeq 120\text{m}$ to $l_2 \simeq 2\text{m}$, then the noise would increase by only a factor

$$\frac{\sqrt{\ln(4000/2)}}{\sqrt{\ln(4000/120)}} \simeq \sqrt{2}. \quad (2)$$

(This assumes that the mirror's scattering probability remains $dP/d\Omega_{\text{bs}} \propto 1/\theta^2$ out to angles of a few tenths of a radian, which it might not.)

The goal of the LIGO baffle design has been to keep the total light-scattering noise below 1/10 the standard quantum limit for a 1 ton test mass in the range 10Hz to 100Hz, i.e. below [1]

$$\tilde{h}_{\text{goal}} = \frac{1}{10} \left(\frac{8\hbar}{m(2\pi fL)^2} \right)^{1/2} = \frac{4 \times 10^{-25} \text{ 10Hz}}{\sqrt{\text{Hz}} f}. \quad (3)$$

Here $m = 1\text{ton}$ is the mass of the test mass.

The baffle-backscatter noise (1) is 3/4 this goal at 10Hz and 3/40 at 100Hz, for our fiducial parameters. The most seriously uncertain parameters are the seismic noise level $\tilde{\xi}_s(f)$ and the amplification factor $\bar{A}(f)$ due to seismic excitations of beam-tube normal modes. The lowest tube normal-mode frequency is $\sim 20\text{Hz}$ [9], so some of the normal modes lie right in the frequency band of greatest concern, 10 to 100Hz. Moreover, originally all the baffles were to have been placed at beam tube supports, thereby avoiding much amplification; in the current design many baffles are not at support points, so amplification has become a serious worry. That worry is mitigated somewhat by the fact (Sec. II C) that only vibrations (nearly) parallel to the beam-tube axis contribute to the noise, and the largest amplifications are likely to be perpendicular to the axis not parallel. Nevertheless, we should be prepared for the possibility that the amplification $\bar{A}(f)$ might be as large as 10, causing a factor 5 failure to achieve the noise goal at 10 Hz. On the other hand, low seismic noise *might* compensate for this: Seismic measurements at the two LIGO sites suggest [5] that $\tilde{\xi}_s(f)$ might be as small as $10^{-8} \text{ cm Hz}^{-1/2} (f/10\text{Hz})^{-2}$ in the 10 to 100 Hz band, i.e. 1/10 the fiducial level used in Eq. (1). There is also uncertainty in the scattering amplitudes α and β and in the angular scaling law for the mirror scattering, and we also worry that coherence effects in the scattering, which are not taken into account in our analysis, might push the noise upward.

In view of these uncertainties and the danger that they may combine to drive the noise (1) significantly above the goal (3), we offer *Recommendation 1: Serious consideration should be given to changing the baffle material to Martin Black or some other material with a comparably low backscatter probability $\beta \lesssim 0.001$.* This change would reduce the scattered-light power by an order of magnitude and correspondingly would reduce $\tilde{h}_{\text{baffles}}$ by a factor 3 at all frequencies. (Vladimir Braginsky informs us that there are various black oxides, including a black chromium oxide, that might have low backscatter probabilities.)

B. Backscatter Off Bare Wall

Backscatter off the bare wall near each mirror was overlooked in Thorne's previous analysis [1], but was included in the scattering simulations by BRO [2]. In Sec. II we compute it analytically.

The scattered light hits and backscatters off the bare wall at an incidence/backscatter angle θ_{bs} that can be as small as $\theta_o \equiv 0.6\text{m}/120\text{m} = 0.005\text{radians} \ll 1$. As we shall see below, the resulting gravitational-wave noise is quite sensitive to how the backscatter probability $dP/d\Omega_{\text{bs}}$ depends on θ_{bs} .

The precise definition of $dP/d\Omega_{\text{bs}}$ is this: Let a beam of light hit the wall at an incident angle θ_{bs} . (If the light comes from a mirror at the center of the beam tube's cross section as in Fig. 1, then θ_{bs} is equal to the angle θ shown in that figure.) Then $dP/d\Omega_{\text{bs}}$ is the probability that any photon in the incident beam will backscatter into a unit solid angle $d\Omega_{\text{bs}}$ centered on the direction back to the mirror. This $dP/d\Omega_{\text{bs}}$ is related to the wall's *bidirectional reflectance distribution function* (BRDF) by [6]

$$\frac{dP}{d\Omega_{\text{bs}}} = \sin \theta_{\text{bs}} \times \text{BRDF}. \quad (4)$$

BRO assumed, in their analysis, that the BRDF is independent of θ_{bs} , and correspondingly that $dP/d\Omega_{\text{bs}} = \beta\theta_{\text{bs}}$ for small θ_{bs} ; and from their scattering measurements at angles ~ 1 for the candidate beam-tube material, they inferred that $\beta \simeq 10^{-2}$. Some consequences of this show up clearly in the BRO report [2]. For example, in the figures on pages 9 and 11 of [2], which depict the intensity $dI/dAd\Omega_{\text{ms}}(\theta)$ [units ergs/(sec cm² ster)] of the light returning to a centered mirror from an angle θ (which BRO call B), there is a sharp drop by a factor $1/\theta_o \simeq 200$ in going from return angles $\theta < \theta_o$ that intercept baffles to return angles $\theta > \theta_o$ that intercept the bare beam-tube wall.

It is far from obvious to us that the walls' BRDF is independent of θ_{bs} for small θ_{bs} . We know of no empirical evidence that favors this over, for example, the more pessimistic assumption that $dP/d\Omega_{\text{bs}}$ is independent of θ_{bs} ; nor have we been able to convince ourselves that theory favors one or the other (or something else in their vicinity), in the walls' regime of (rms roughness) $\equiv \sigma \sim 10\lambda$. [In Appendix A, we discuss the predictions and domains of validity of the standard theories used to calculate the BRDF, and we point out a number of reasons why the standard theories may fail for the LIGO beam tubes in the relevant regime of $0.005 \lesssim \theta_{\text{bs}} \lesssim 0.1$ and $\sigma = 10\lambda$.]

For these reasons, we believe it would be unwise either (i) to accept the BRO assumption $dP/d\Omega_{\text{bs}} \propto \theta_{\text{bs}}$, or (ii) to rely on theory (which predicts in some regimes exponentially small backscatter at grazing incidence [9,10]) to tell us the angular dependence of $dP/d\Omega_{\text{bs}}$. We must be prepared for the possibility that $dP/d\Omega_{\text{bs}}$ is independent of θ , for example, rather than being proportional to

θ as assumed by BRO; and as we shall see below, these two possibilities lead to significantly different noise levels, with different recommendations for the baffling. These differences motivate our

Recommendation 2: The backscatter probability $dP/d\Omega_{\text{bs}}$ should be measured for the LIGO wall material at small angles, $0.005 \lesssim \theta \lesssim 0.1$. [As an important side issue, we make *Recommendation 3:* The specular reflectivity plus forward scattering of the wall material should also be measured for this same range of angles, to test the assumption that the reflectivity plus forward scattering is high for $\theta \lesssim 0.01$ but falls sharply as θ increases above this value; this assumption and the details of the falloff are crucial to the present choice of where to place the first baffle, and as we discuss in Appendix A, the theory of the falloff is not fully reliable.]

Since we do not know the actual angular dependence of the wall's backscatter probability, in Sec. II we evaluate the gravity-wave noise under two fiducial assumptions: $dP/d\Omega_{\text{bs}} = \beta \simeq 0.01$ which we shall call *pessimistic*, and ($dP/d\Omega_{\text{bs}} = \beta\theta$), which we shall call *optimistic*.

In the *pessimistic case*, our calculations give a wall-noise formula identical to that, Eq. (1), for baffle noise; and the formula and numbers are identical to what would result if the near wall were fully baffled instead of being left bare, and are essentially the same as the noise from the now-planned baffle configuration:

$$\begin{aligned} \tilde{h}(f) &= \left[4\pi\alpha^2\beta \ln\left(\frac{l_1}{l_2}\right) J_0(\rho) \right]^{1/2} \bar{A}(f) \frac{\lambda}{R} \frac{\tilde{\xi}_s(f)}{L} \\ &= \frac{3 \times 10^{-25}}{\text{Hz}^{1/2}} \left(\frac{10\text{Hz}}{f}\right)^2 \bar{A}(f) \frac{\sqrt{J_0(\rho)}}{2} \frac{\alpha}{10^{-6}} \left(\frac{\beta}{0.01}\right)^{1/2} \\ &\quad \times \left(\frac{\ln(l_1/l_2)}{\ln(120\text{m}/2\text{m})}\right)^{1/2} \frac{\tilde{\xi}_s(f)}{10^{-7}\text{cmHz}^{-1/2}(f/10\text{Hz})^{-2}}; \end{aligned} \quad (5)$$

cf. the paragraph following Eq. (33). Here the notation is the same as in Eq. (1), except that now l_1 is the distance to the end of the bare wall ($\simeq 120\text{m}$) rather than to the end of the baffles, and l_2 is the distance to the beginning of the bare wall ($\simeq 2\text{m}$) rather than to the beginning of the baffles. Because the wall noise (5) and baffle noise (1) are incoherent with respect to each other, they add in quadrature; the net noise is $\sqrt{2}$ times that of either the wall or the baffles alone.

If this pessimistic case is correct, then wall backscatter presents the same dangers as baffle backscatter: the tube-vibration amplification factor $\bar{A}(f)$ might be as large as 10, and other parameters might be larger than our estimates, thereby seriously violating the noise goal (3). A factor 3 improvement can be achieved in the case of baffle noise by changing the baffle material to Martin black or something like it. To achieve the same factor 3 improvement for wall noise (in the pessimistic case), it will be necessary to baffle the nearby wall with Martin black. Thus, we are led to *Recommendation 4: Pending*

measurements of $dP/d\Omega_{\text{bs}}$ in the range $0.005 \lesssim \theta \lesssim 0.1$, serious consideration should be given to extending the beam-tube baffling up to the test mass vacuum chamber instead of beginning it only $\simeq 120$ meters down the tube as now planned.

In the *optimistic case* $dP/d\Omega_{\text{bs}} = \beta\theta_{\text{bs}}$, our calculations give [Eq. (34)]

$$\begin{aligned} \tilde{h}(f) &= [4\pi\alpha^2\beta\theta_2 J_1(\rho)]^{1/2} \bar{A}(f) \frac{\lambda}{R} \frac{\tilde{\xi}_s(f)}{L} \\ &= \frac{0.8 \times 10^{-25}}{\text{Hz}^{1/2}} \left(\frac{10\text{Hz}}{f}\right)^2 \bar{A}(f) \frac{\sqrt{J_1(\rho)}}{1.5} \left(\frac{\beta}{0.01}\right)^{1/2} \\ &\quad \times \left(\frac{\theta_2}{0.5}\right)^{1/2} \frac{\tilde{\xi}_s(f)}{10^{-7}(f/10\text{Hz})^{-2}}. \end{aligned} \quad (6)$$

Here the notation is as in Eq. (1), with two exceptions: $\theta_2 = l_2/R \sim 0.5$ is the angle of incidence/backscatter at the nearest location on the bare wall for the case of mirrors at the center of the beam-tube cross section, and the function $J_1(\rho)$ describing the effects of offsetting the mirror from the tube center is a little different from the $J_0(\rho)$ of Eqs. (1) and (5) (it is the curve labeled $n = 1$ in Fig. 3 rather than $n = 0$).

The dependence on the distance $l_2 = R\theta_2$ to the beginning of the beam tube is indicative of the fact that, in this optimistic case, the most serious noise comes from the nearest portions of the tube. This reminds us of the importance of controlling scattered light from surfaces even closer, in the test-mass chambers.

A comparison of Eq. (6) with Eqs. (3) and (1) shows that in this optimistic case $dP/d\Omega_{\text{bs}} \propto \theta_{\text{bs}}$, the bare-wall noise is adequately far below the scattered-noise goal, and baffling the nearby wall with Martin black would not reduce it further.

C. Backscatter Off Objects at the Far End of the Beam Tube

Since the mirror scattering is so sharply peaked toward small angles $\theta \ll 1$, we must pay attention to light scattered into the far end of the beam tube (angles $\theta \lesssim R/L \simeq 1.5 \times 10^{-4}$, but $\theta > R_{\text{mirror}}/L \simeq 3 \times 10^{-5}$ so the light misses the far mirror). This light can backscatter off the walls of the far test-mass chamber or off objects in it, and return to the originating mirror to produce gravity-wave noise.

We have evaluated the resulting noise spectrum under the following assumptions: (i) The backscattering surfaces have the same backscatter probability as the baffles, $dP/d\Omega_{\text{bs}} = \beta \simeq 0.01$. (ii) The backscattering surfaces vibrate longitudinally with the same noise spectrum as the baffles $\xi(f) = A(f)\tilde{\xi}_s(f)$. (iii) The backscattering surfaces subtend the entire area of the beam tube's end, except that of the end mirror. (iv) The mirror's scattering probability retains the same form $dP/d\Omega_{\text{ms}} = \alpha/\theta^2$ in the far-end region $3 \times 10^{-5} \lesssim \theta \lesssim 1.5 \times 10^{-4}$ as it

has in the baffle region $\theta \gtrsim 1.5 \times 10^{-4}$. This fourth assumption may be overly optimistic: measurements of a sample mirror [3] suggest that at the tiny scattering angles $3 \times 10^{-5} \lesssim \theta \lesssim 1.5 \times 10^{-4}$, the scattering probability might be enhanced over the $1/\theta^2$ form.

These assumptions lead to the following noise spectrum [cf. Eq. (36) and associated discussion]

$$\begin{aligned} \tilde{h}(f) &= \sqrt{2\pi\alpha^2\beta}\bar{A}(f)\frac{\lambda}{R_{\text{mirror}}}\frac{\tilde{\xi}_s(f)}{L} \\ &= \frac{3 \times 10^{-25}}{\text{Hz}^{1/2}} \left(\frac{10\text{Hz}}{f}\right)^2 \frac{\alpha}{10^{-6}} \left(\frac{\beta}{0.01}\right)^{1/2} \bar{A}(f) \\ &\quad \times \frac{\tilde{\xi}_s(f)}{10^{-7}\text{cmHz}^{-1/2}(f/10\text{Hz})^{-2}}. \end{aligned} \quad (7)$$

Here $R_{\text{mirror}} \simeq 12\text{cm}$ is the mirror radius. Note that for mirrors at the center of the beam tube ($\rho = 0$), this scattering noise is twice as large as that (1) due to the baffles, and for mirrors 2/3 of the way to the beam-tube wall ($\rho = 2/3$), it is the same as the baffle noise. This leads to our *Recommendation 5: When instrumenting and baffling each test-mass chamber, careful attention should be paid to backscattering of light that arrives from test-mass mirrors at the opposite end of the beam tube.*

II. DERIVATION OF NOISE SPECTRA

In this section we derive the noise spectra (1), (5) and (6) quoted above, including their dependence on the various parameters and scattering probabilities. Our derivations are via a more direct route than was used in Thorne's previous report [1].

The backscatter processes are sufficiently simple that the following analysis should be quite reliable and accurate, modulo the (considerable) uncertainties in various parameters and the scattering probabilities.

A. Gravity-Wave Noise in Terms of Scattered Light Returned to Main Beam

In this subsection we shall derive a general expression for the gravitational-wave noise spectrum $\tilde{h}^2(f)$ in terms of the power and spectrum of the light scattered back into the interferometer's main beam. To simplify our derivation, we shall pretend that the gravity-wave signal is all produced in just one of the interferometer's two arms. In other words, we shall take the true gravity-wave signal, which is deposited partially in arm 1 and partially in arm 2 (with the division between arms depending on the direction to the source and on the signal's polarization), and shall computationally put the entire signal into arm 1. Then we shall use that arm-1 signal as a tool in computing, in gravity-wave units, the scattered-light noise produced in arm 1; and finally we shall assert (as should

be obvious) that the same amount of noise power must be produced in arm 2 as in arm 1.

When the gravitational wave $h(t)$ interacts with the interferometer, exerting its entire force on arm 1, it displaces the end test mass of arm 1 by an amount $\delta L = h(t)L$ relative to the corner test mass, where $L = 4\text{km}$ is the arm length; and it does nothing to arm 2. If ψ_{mb} is the main-beam electric field in arm 1 impinging on the end mass's mirror, then the displacement δL induces a phase shift $2k\delta L \ll 1$ on the main-beam light (where $k = 2\pi/\lambda$ is the light's wave number). The gravity wave thereby augments onto the main beam the new field $\delta\psi_{\text{mb}} = i2k\delta L\psi_{\text{mb}} = i(2kL)h\psi_{\text{mb}}$; i.e.,

$$\frac{\delta\psi_{\text{mb}}}{\psi_{\text{mb}}} = i(2kL)h. \quad (8)$$

When light scatters off one of the test-mass mirrors, then backscatters off some small region of a vibrating baffle or bare wall thereby acquiring a phase shift $\Phi(t)$, then hits the mirror again and scatters back into the main beam, it augments onto the main beam a new field $\delta\psi_{\text{mb}}$ given by

$$\frac{\delta\psi_{\text{mb}}}{\psi_{\text{mb}}} = \left(\frac{\delta I_{\text{mb}}}{I_{\text{mb}}}\right)^{1/2} e^{i\Phi} = \left(\frac{\delta I_{\text{mb}}}{I_{\text{mb}}}\right)^{1/2} (\cos\Phi + i\sin\Phi). \quad (9)$$

Here I_{mb} is the power (ergs/sec) of the light in the main beam, and δI_{mb} is the rate (ergs/sec) at which the scattered light is returning to the main beam.

By comparison with Eq. (8) we see that the imaginary part of expression (9) simulates the effect of a gravitational wave; the simulated wave field is obviously

$$h(t) = \left(\frac{\delta I_{\text{mb}}}{I_{\text{mb}}}\right)^{1/2} \frac{\mathcal{S}(t)}{2kL}, \quad (10)$$

where

$$\mathcal{S}(t) \equiv \sin[\Phi(t)]. \quad (11)$$

Since $\Phi(t)$ fluctuates randomly, so does $\mathcal{S}(t)$ and thence $h(t)$. Equation (10) implies that the spectral density of the resulting gravity-wave noise is related to that of \mathcal{S} by

$$\delta\tilde{h}^2(f) = \frac{\delta I_{\text{mb}}}{I_{\text{mb}}} \left(\frac{\lambda}{4\pi L}\right)^2 \tilde{\mathcal{S}}^2(f). \quad (12)$$

Here we have used $k = 2\pi/\lambda$.

To reiterate, Eq. (12) is the gravity-wave noise spectrum expressed in terms of the the total power I_{mb} of the main beam in arm 1, the power δI_{mb} of backscattered light returning to the main beam from some small region of a baffle or bare tube wall, the spectral density $\tilde{\mathcal{S}}^2(f)$ of the sine of the phase fluctuations of this scattered light, the light wavelength $\lambda = 4 \times 10^{-5}\text{cm}$, and the arm length $L = 4\text{km}$. Because the baffles and wall

are randomly rough, the backscattered light from different locations will superpose incoherently when it returns to the main beam, with light from each region having a possibly different spectral shape $\tilde{S}^2(f)$. To compute the total noise spectrum $\tilde{h}^2(f)$, we must add up the contributions $\delta\tilde{h}^2(f)$ [Eq. (12)] from all regions of backscatter, including backscatter onto all four mirrors of the interferometer (since as noted earlier an equal amount of noise power is produced at the mirrors of arm 2 as at those of arm 1).

B. Rate of Addition of Light to Main Beam, and Resulting Noise

Main-beam light, hitting one of an arm's mirrors, scatters off it toward the baffles or bare wall at a rate governed by the scattering probability per unit solid angle $dP/d\Omega_{\text{ms}}$. (The subscript "ms" stands for "mirror scattering".) This probability depends on the direction into which the light is scattered, and it is defined by the relation

$$\frac{dI}{d\Omega_{\text{ms}}} = I_{\text{mb}} \frac{dP}{d\Omega_{\text{ms}}}. \quad (13)$$

Here I_{ms} is the main-beam power, and $dI/d\Omega_{\text{ms}}$ is the energy scattered per unit time into a unit solid angle $d\Omega_{\text{ms}}$ about the direction of interest; cf. Fig. 1. (We do not, until the end of this subsection, assume that the scattering is axisymmetric, i.e. that it depends only on the angle θ of the chosen direction to the main beam.)

Consider the light scattered into a tiny solid angle $\delta\Omega_{\text{ms}}$ around the direction of interest. Each photon of this light has some probability $dP/d\Omega_{\text{bs}}$ of scattering back toward the mirror, in a unit solid angle $d\Omega_{\text{bs}}$. The value of this backscatter probability depends on whether the photon hits a baffle, or hits the bare wall; and if it hits the wall, the probability may also depend on the photon's incidence angle (which must equal the backscatter angle since the photon is required to return to the mirror). The total energy flux ($\text{erg cm}^{-2} \text{ s}^{-1}$) returning back to the mirror from the tiny solid angle $\delta\Omega_{\text{ms}}$ is obviously

$$\left(\frac{d\delta I}{dA}\right) = I_{\text{mb}} \frac{dP}{d\Omega_{\text{ms}}} \delta\Omega_{\text{ms}} \frac{dP}{d\Omega_{\text{bs}}} \frac{1}{r^2}, \quad (14)$$

where r is the distance between the mirror and the location of backscatter.

There is a certain cross section σ_{ms} for the mirror to scatter this impinging light flux back into the main beam. If we multiply expression (14) by this cross section, we obtain the rate (ergs/sec) that the solid angle $\delta\Omega_{\text{ms}}$ is sending backscattered light into the main beam:

$$\delta I_{\text{mb}} = I_{\text{mb}} \frac{dP}{d\Omega_{\text{ms}}} \delta\Omega_{\text{ms}} \frac{dP}{d\Omega_{\text{bs}}} \frac{1}{r^2} \sigma_{\text{ms}}. \quad (15)$$

Not surprisingly, there is a reciprocity relation that links the mirror's probability per unit solid angle $dP/d\Omega_{\text{ms}}$ to

scatter a photon out of the main beam and into the direction of interest, and the cross section σ_{ms} for that same mirror to scatter an incoming photon from that same direction back into the main beam. That reciprocity relation is given by

$$\sigma_{\text{ms}} = \lambda^2 \frac{dP}{d\Omega_{\text{ms}}}, \quad (16)$$

where λ is the wavelength of the light. We derive this relation in Appendix B.

By combining this reciprocity relation with Eq. (15), we obtain the following very general expression for the rate at which energy is scattered back into the main beam from a tiny solid angle $\delta\Omega_{\text{ms}}$ in any direction of interest:

$$\frac{\delta I_{\text{mb}}}{I_{\text{mb}}} = \frac{\lambda^2}{r^2} \left(\frac{dP}{d\Omega_{\text{ms}}}\right)^2 \frac{dP}{d\Omega_{\text{bs}}} \delta\Omega_{\text{ms}}. \quad (17)$$

By then inserting expression (17) into (12), we obtain the following formula for the noise produced by the light that backscatters from the tiny solid angle $\delta\Omega_{\text{ms}}$:

$$\delta\tilde{h}^2(f) = \left(\frac{\lambda}{r}\right)^2 \left(\frac{\lambda}{4\pi L}\right)^2 \left(\frac{dP}{d\Omega_{\text{ms}}}\right)^2 \frac{dP}{d\Omega_{\text{bs}}} \tilde{S}^2(f) \delta\Omega_{\text{ms}}. \quad (18)$$

To reiterate: $\delta\tilde{h}^2(f)$ is the contribution to the spectral density of gravity-wave noise produced by light that scatters off a mirror into the tiny solid angle $\delta\Omega_{\text{ms}}$, $dP/d\Omega_{\text{ms}}$ is the mirror's probability to scatter main-beam photons into a unit solid angle in the direction of $\delta\Omega_{\text{ms}}$, r is the distance from the mirror to the backscatter surface along the direction of $\delta\Omega_{\text{ms}}$, $dP/d\Omega_{\text{bs}}$ is the probability for a photon arriving at the backscatter surface to get backscattered into a unit solid angle in the direction of the mirror, $\tilde{S}^2(f)$ is the spectral density of the sine of the phase fluctuations Φ put onto the light by vibrations of the backscatter surface, λ is the wavelength of the light, L is the length of an interferometer arm; and the total noise is obtained by adding up expression (18) over all scattering solid angles $\delta\Omega_{\text{ms}}$ for all four mirrors of the interferometer.

In the following subsections we shall assume, for simplicity, that the mirror is at the center of the beam tube's cross section and that it scatters light axisymmetrically so $dP/d\Omega_{\text{ms}}$ is a function only of θ , the angle between the scattered-light direction and the main beam (Fig. 1). (In Appendix C we shall treat mirrors that are offset from the center of the beam tube.) Similarly, we shall assume that the beam tube's backscattering is axisymmetric, so $dP/d\Omega_{\text{bs}}$ and $\tilde{S}^2(f)$ depend only on θ , the angle of the scattered-light rays to the main beam, i.e. to the axis of symmetry. Note that this axisymmetry implies [aside from small corrections of order (baffle height)/(beam tube radius R), which we shall ignore] that the distance r from the mirror to the backscatter surface is $R/\sin\theta \simeq R/\theta$. We shall also assume that the four

mirrors have the same scattering probability $dP/d\Omega_{\text{ms}}$ and see walls and baffles with the same backscatter probabilities $dP/d\Omega_{\text{bs}}$.

With these assumptions and using $\theta \ll 1$, the total noise spectrum produced by all the backscattered light [the sum of (18) over all solid angles $\delta\Omega_{\text{ms}}$] becomes

$$\tilde{h}^2(f) = \left(\frac{\lambda}{R}\right)^2 \left(\frac{\lambda}{4\pi L}\right)^2 \times \int_{\theta_1}^{\theta_2} \left(\frac{dP(\theta)}{d\Omega_{\text{ms}}}\right)^2 \frac{dP(\theta)}{d\Omega_{\text{bs}}} \tilde{S}^2(f, \theta) 8\pi\theta^3 d\theta. \quad (19)$$

The constant in the integration element is 8π rather than 2π because we must integrate over the light scattered from four mirrors, not just one. The limits of integration for the entire 60cm-radius beam tube beyond the gate valve (Fig. 1) are $\theta_1 = R/L = 60\text{cm}/4\text{km} = 1.5 \times 10^{-5}$ and $\theta_2 \simeq (60\text{cm}/20\text{m}) = 0.03$; and similarly for the 90cm-radius section of beam tube (Fig. 1).

C. Phase Shift Produced by Backscatter

The light scattered off a mirror into some tiny solid angle $\delta\Omega_{\text{ms}}$ hits and backscatters off some small portion of a beam tube wall or baffle. By its vibrations, that “backscatter surface” puts a time-varying phase shift $\Phi(t)$ onto the backscattered light. We shall resolve the surface’s vibrational displacement $\vec{\xi}(t)$ into a scalar component ξ_{\parallel} parallel to the incoming and backscattered light rays, and a vectorial component $\vec{\xi}_{\perp}$ perpendicular to the rays; see Fig. 2.

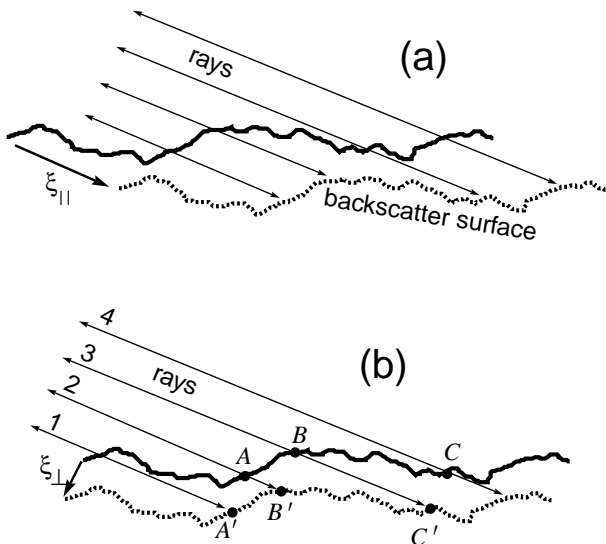


FIG. 2. Backscatter of light off a small portion of a vibrating baffle or beam-tube wall.

The parallel displacement ξ_{\parallel} lengthens each round-trip ray by $2\xi_{\parallel}$ (cf. Fig. 2a), thereby putting onto the light a phase shift

$$\Phi_{\parallel} = 2k\xi_{\parallel} = 4\pi\frac{\xi_{\parallel}}{\lambda}. \quad (20)$$

The perpendicular displacement $2\vec{\xi}_{\perp}$ lengthens the various rays by different amounts (Fig. 2b), but the average lengthening is $2\xi_{\perp}^n / \sin\theta$, which can be far larger than $|\vec{\xi}|$ for $\theta \ll 1$. (Here ξ_{\perp}^n is the projection of $\vec{\xi}_{\perp}$ into a plane that is normal to the smoothed (averaged) backscatter surface and parallel to the rays.) At first sight one might expect (as we did) that this average ray lengthening will produce a phase shift $\Phi_{\perp} = 2k\xi_{\perp}^n / \sin\theta$ on the backscattered light. As Stan Whitcomb has pointed out to us, this is not so; and, in fact, the true phase shift Φ_{\perp} is negligible compared to that Φ_{\parallel} due to the parallel displacement.

To understand why, consider first the idealized situation where the incoming light is precisely planar. Then the displacement $\vec{\xi}_{\perp}$ is equivalent to mapping ray 1 of Fig. 2b into ray 2, and ray 2 into ray 3, and ray 3 into ray 4, so point A gets mapped into A' , B into B' , and C into C' . Because the incoming light is planar, it is unchanged by this mapping; i.e., all the rays are equivalent. Therefore, the backscattered light must be completely unchanged by this mapping, except for a transverse displacement everywhere by $\vec{\xi}_{\perp}$. Since the magnitude of this displacement is $\lesssim 0.01\mu\text{m}$ and the backscattered light, upon reaching the mirror, varies in amplitude and phase only on scales \gtrsim (Fresnel length) $\equiv \sqrt{\lambda r} \gtrsim 1\text{mm}$ (where $r > 1\text{m}$ is the distance between backscatter surface and mirror), the fractional displacement-induced change in the scattered light’s phase is

$$\Phi_{\perp} \lesssim \frac{|\vec{\xi}_{\perp}|}{\sqrt{\lambda r}} \lesssim \frac{0.01\mu\text{m}}{1\text{mm}} = 10^{-5}. \quad (21)$$

Now, the incoming light at the backscatter surface is not truly planar. However, since it originated at the mirror a distance r away, it can vary significantly in phase only on lengthscales $\gtrsim \sqrt{\lambda r}$; and correspondingly, the perpendicular surface displacement changes the phase of the incoming light, as seen at a fixed point on the backscatter surface (e.g. $A = A'$), by an amount no larger than Eq. (21); and this in turn will put a phase shift on the backscattered light no larger than (21). Thus, Eq. (21) is an approximate upper bound on the net phase shift produced by the backscatter surface’s perpendicular displacement.

The ratio of the phase shifts induced by displacements perpendicular and parallel to the incoming rays [Eqs. (21) and (20)] is

$$\frac{|\Phi_{\perp}|}{|\Phi_{\parallel}|} \lesssim \frac{\sqrt{\lambda/r} |\vec{\xi}_{\perp}|}{4\pi |\xi_{\parallel}|} \ll 1, \quad (22)$$

since $|\vec{\xi}_\perp|/|\xi_\parallel| \sim 1$. Therefore, the parallel phase shift dominates, and the net phase shift is

$$\Phi = \Phi_\parallel = 4\pi \frac{\xi_\parallel}{\lambda}. \quad (23)$$

The displacement ξ_\parallel is produced by seismic motions of the ground beneath the beam tube. Consequently, the scattering surface will vibrate with a spectrum

$$\tilde{\xi}_\parallel(f) = A(f)\xi_s(f), \quad (24)$$

where

$$\tilde{\xi}_s(f) \sim \frac{10^{-7} \text{ cm}}{\sqrt{\text{Hz}}} \left(\frac{10 \text{ Hz}}{f} \right)^2 \quad (25)$$

is the spectrum of horizontal seismic motions and $A(f)$ is an amplification factor, due to seismic excitations of the beam-tube normal modes. The amplification $A(f)$ will vary from one location on the beam tube to another, but presumably at most locations it will fall in the range ~ 1 to ~ 10 .

By combining Eqs. (23) and (24), we obtain for the spectrum of the backscattered light's phase fluctuations

$$\tilde{\Phi}(f) = 4\pi A(f) \frac{\tilde{\xi}_s(f)}{\lambda}. \quad (26)$$

The gravity-wave noise is proportional to $\mathcal{S}(t) \equiv \sin[\Phi(t)]$, where the zero of phase, by convention, is displaced $\pi/2$ from the phase of the main-beam light. The backscattered light's absolute phase, with this convention, consists of a piece Φ_{slow} that varies slowly with time (at $f \ll 10\text{Hz}$) and also varies from one region of the beam-tube wall or baffle to another, plus a piece Φ_{fast} that varies in the frequency band of interest, $f \gtrsim 10\text{Hz}$: $\Phi = \Phi_{\text{slow}} + \Phi_{\text{fast}}$. Correspondingly,

$$\mathcal{S} = \sin(\Phi_{\text{slow}} + \Phi_{\text{fast}}) \simeq \sin(\Phi_{\text{slow}}) + \cos(\Phi_{\text{slow}})\Phi_{\text{fast}}, \quad (27)$$

where we have used the fact that the rms fluctuations of Φ_{fast} are small compared to unity. The spectral density of this \mathcal{S} at the fast frequencies of interest is

$$\tilde{\mathcal{S}}^2(f) = \langle \cos^2(\Phi_{\text{slow}}) \rangle \tilde{\Phi}_{\text{fast}}^2(f) = 8\pi^2 A^2(f) \frac{\tilde{\xi}_s^2(f)}{\lambda^2}, \quad (28)$$

where we have used the value $\langle \cos^2(\Phi_{\text{slow}}) \rangle = 1/2$ for $\cos^2(\Phi_{\text{slow}})$ averaged over time and over locations on the scattering surface, and have used Eq. (26) for $\tilde{\Phi}_{\text{fast}}$.

D. Noise Spectrum for Light Backscattered from Baffles

For concrete evaluations of the noise spectrum, we shall assume a mirror scattering probability [1,3]

$$\frac{dP}{d\Omega_{\text{ms}}} = \frac{\alpha}{\theta^2} \quad \text{with } \alpha = 10^{-6}. \quad (29)$$

The baffles are inclined at a 35° angle to the beam-tube wall, so the incidence and backscatter angles are $\theta_B = 35^\circ + \theta \simeq 35^\circ$. Since θ_B is essentially independent of θ , we can treat the baffles' backscatter probability as a constant, the same for all regions of all baffles, which we will denote β :

$$\left(\frac{dP}{d\Omega_{\text{bs}}} \right)_{\text{baffle}} = \beta. \quad (30)$$

If the baffles are made from the same material as the beam tube, as currently planned, then $\beta \simeq 0.01$ [4]; if they are made from Martin Black, then $\beta \simeq 0.001$ [8].

By inserting Eqs. (28), (29) and (30) into (19), performing the integral, and taking the square root, we obtain the following baffle-backscatter-induced noise spectrum:

$$\begin{aligned} \tilde{h}(f) &= \left[4\pi\alpha^2\beta \ln\left(\frac{l_1}{l_2}\right) J_0(\rho) \right]^{1/2} \bar{A}(f) \frac{\lambda}{R} \frac{\tilde{\xi}_s(f)}{L} \\ &= \frac{3 \times 10^{-25}}{\text{Hz}^{1/2}} \left(\frac{10 \text{ Hz}}{f} \right)^2 \bar{A}(f) \frac{\sqrt{J_0(\rho)}}{2} \left(\frac{\beta}{0.01} \right)^{1/2} \\ &\quad \times \left(\frac{\ln(l_1/l_2)}{\ln(4\text{km}/120\text{m})} \right)^{1/2} \frac{\tilde{\xi}_s(f)}{10^{-7} \text{ cm Hz}^{-1/2} (f/10\text{Hz})^{-2}}. \end{aligned} \quad (31)$$

Here $l_1 = 4\text{km}$ and $l_2 \simeq 120\text{m}$ are the distances from the mirror to the farthest and nearest baffles, $\bar{A}(f)$ is the mean baffle vibration amplification factor (suitably averaged over all baffles), and we have inserted a function $J_0(\rho)$ which deals with the possibility (not included in the above calculation) that the mirrors are offset from the center of the beam tube. This $J_0(\rho)$ is derived in Appendix C; its argument ρ is the fraction of the tube radius by which the mirrors are offset, and its value varies from $J_0(0) = 1$ for mirrors at the tube center to $J_0(2/3) = 3.3$ for mirrors $2/3$ of the way to the edge of the tube (about as near the edge as mirrors are likely to be placed).

The second and third lines of Eq. (31) are the spectrum quoted and discussed in Sec. I [Eq. (1)]. The parameters contained therein correspond to the present baffle design. By switching from wall material for the baffles ($\beta = 0.01$) to Martin Black ($\beta = 0.001$), we can reduce the baffle noise by $1/\sqrt{10} \simeq 1/3$. If the baffles extend all the way in to the test-mass chamber instead of beginning $\simeq 120\text{m}$ down the tube, the logarithmic term increases by about a factor 2, so the baffle noise \tilde{h} goes up by $\sqrt{2} \simeq 1.4$.

E. Noise Spectrum for Light Backscattered from Bare Tube Wall

As was noted in Sec. I.A, the wall's backscatter probability $dP/d\Omega_{\text{bs}}$ is not known at the small incidence/backscatter angles θ of concern to us. Accordingly, we shall explore the consequences of two possibilities:

$$\frac{dP}{d\Omega_{\text{bs}}} = \beta = 0.01 \quad \text{“pessimistic,”} \quad (32)$$

$$\frac{dP}{d\Omega_{\text{bs}}} = \beta\theta = 0.01\theta \quad \text{“optimistic.”} \quad (33)$$

In both cases we take $\beta = 0.01$ in accord with BRO measurements at large incidence angles θ [4]. By inserting Eqs. (28), (29), and (32) or (33) into (19), performing the integral, and taking the square root, we obtain the wall-backscatter-induced noise spectrum.

For the pessimistic case, $dP/d\Omega_{\text{bs}} = \beta$, the spectrum is identical to that for baffles, Eq. (31), but with the distances in the logarithm changed to $l_1 =$ (distance from mirror to end of bare wall) $\simeq 120\text{m}$ and $l_2 =$ (distance from mirror to beginning of bare wall) $\simeq 1.2\text{m}$.

For the optimistic case, the $\ln(l_1/l_2) = \ln(\theta_2/\theta_1)$ term in (31) gets replaced by $\theta_2 - \theta_1 \simeq \theta_2 = R/l_2$ and the $J_0(\rho)$ gets replaced by a slightly different function, $J_1(\rho)$ (Appendix C), so

$$\begin{aligned} \tilde{h}(f) &= [4\pi\alpha^2\beta\theta_2J_1(\rho)]^{1/2} \bar{A}(f) \frac{\lambda}{R} \frac{\tilde{\xi}_s(f)}{L} \\ &= \frac{0.8 \times 10^{-25}}{\text{Hz}^{1/2}} \left(\frac{10\text{Hz}}{f}\right)^2 \bar{A}(f) \frac{\sqrt{J_1(\rho)}}{1.5} \left(\frac{\beta}{0.01}\right)^{1/2} \\ &\quad \times \left(\frac{\theta_2}{0.5}\right)^{1/2} \frac{\tilde{\xi}_s(f)}{10^{-7}(f/10\text{Hz})^{-2}} \end{aligned} \quad (34)$$

Note that the noise is dominated by the portion of the beam-tube wall closest to the mirror.

These are the spectra quoted and discussed in Sec. I [Eqs. (5) and (6)].

F. Noise Spectrum for Light Backscattered from Far End of Beam Tube

Turn, now, to light backscattered from objects at the far end of the beam tube. We assume that the mirror’s scattering law retains the form $dP/d\Omega_{\text{ms}} = \alpha/\theta^2$ at the tiny angles θ of the tube’s far end, and that all surfaces encountered there backscatter with the same probability as the baffles, $dP/d\Omega_{\text{bs}} = \beta \simeq 0.01$, and vibrate longitudinally with the same displacement spectrum as the baffles, $\xi(f) = A(f)\tilde{\xi}_s(f)$. By inserting these assumptions and Eq. (28) into Eq. (18) and integrating over solid angle, we obtain the following expression for the scattering noise:

$$\tilde{h}^2(f) = 2\alpha^2\beta \frac{\lambda^2}{L^2} \frac{\tilde{\xi}_s^2}{L^2} \int A^2\theta^{-4} d\Omega_{\text{ms}}. \quad (35)$$

If the mirrors are centered in the beam tube, then the integral is over an annulus of solid angles ranging from $\theta_1 = R_{\text{mirror}}/L \simeq 3 \times 10^{-5}$ to $\theta_2 = R/L \simeq 1.2 \times 10^{-4}$; and the result (ignoring $1/\theta_2^2$ compared to $1/\theta_1^2$) is

$$\begin{aligned} \tilde{h}(f) &= \sqrt{2\pi\alpha^2\beta} \bar{A}(f) \frac{\lambda}{R_{\text{mirror}}} \frac{\tilde{\xi}_s(f)}{L} \\ &= \frac{3 \times 10^{-25}}{\text{Hz}^{1/2}} \left(\frac{10\text{Hz}}{f}\right)^2 \frac{\alpha}{10^{-6}} \left(\frac{\beta}{0.01}\right)^{1/2} \bar{A}(f) \\ &\quad \times \frac{\tilde{\xi}_s(f)}{10^{-7}\text{cmHz}^{-1/2}(f/10\text{Hz})^{-2}}. \end{aligned} \quad (36)$$

This is the spectrum quoted in Eq. (7).

If the mirrors are displaced from the beam-tube center by a fraction ρ of the tube’s radius, then the solid-angle integral in (35) gives expression (36) multiplied by

$$\left(1 - \frac{R_{\text{mirror}}^2}{R^2} J_0(\rho)\right)^{1/2}; \quad (37)$$

cf. Appendix C. Numerically, this correction is within a few percent of unity for all relevant ρ , which is why we have omitted it in Eq. (7).

ACKNOWLEDGMENTS

We thank Jean-Yves Vinet, Rainer Weiss, and Stan Whitcomb for a number of very helpful conversations and e-mail exchanges. This research was supported by NSF grant PHY-9213508.

APPENDIX A: DOMAIN OF VALIDITY OF THEORETICAL CALCULATIONS OF THE BRDF

There are two well known theories that have been used to calculate the BRDF or equivalently the scattering probability $dP/d\Omega$ for rough surfaces, as a function of the incoming and outgoing angles, and in terms of the spectrum of surface height fluctuations. The first is the smooth-surface theory which is valid when the rms surface roughness σ is small compared to a wavelength. This is the theory used to predict the scattering from mirrors; see, e.g. [6,3]. It does not apply to scattering off the beam tube walls for which $\sigma \simeq 10\lambda$.

The second is the rough-surface theory developed by Beckmann and Spizzichino [7], which requires for its validity that the radii of curvature of the scattering surface be large compared to a wavelength. The predictions of this theory have been summarized by Weiss [10]. There are two different limits of the Beckmann-Spizzichino theory, depending on the Rayleigh roughness parameter [10]

$$g = \left[\frac{4\pi\sigma \sin(\theta_{\text{bs}})}{\lambda} \right]^2, \quad (A1)$$

the “smooth” limit $g \ll 1$ and the “rough” limit $g \gg 1$. For backscattering off the tube wall, the transition between the two limits is at a distance from the mirror of $z \sim 80\text{m}$.

The rough limit is relevant to backscatter from the nearby tube wall. In this limit the Beckmann-Spizzichino theory reduces to a geometric optics theory of light reflecting specularly off a surface with a distribution of local surface slopes. If we assume that $\tau \lesssim \sigma$, where τ is the transverse lengthscale over which the surface height fluctuations become uncorrelated, then in the rough limit the theory predicts that the backscatter is exponentially small at small backscatter angles [10]. However, there are two reasons why the theory may fail in this regime: (i) As pointed out by Weiss [9], the statistical properties of the surface height fluctuations are assumed to be Gaussian, and this may not be the case. [Gaussian surface height fluctuations do not imply a Gaussian surface autocovariance function; the rough limit of the Beckmann-Spizzichino theory is valid for any choice of autocorrelation function.] (ii) If there is significant power in the spectrum of surface fluctuations on scales comparable to a wavelength, the theory will be invalid. It is not known whether this is the case or not for the beam tube walls. [The Beckmann-Spizzichino theory typically does not agree very well quantitatively with experimental measurements of surface autocovariance functions and surface BRDF's [6].]

In the smooth regime $g \ll 1$, there are, in addition to the above, other reasons why the theory may be invalid: (iii) Shadowing of one part of the surface by another is not taken into account and may be important. In fact we would expect shadowing to become more and more important in the limit $\theta_{\text{bs}} \rightarrow 0$. (iv) the usual criterion for the validity of the theory is that $r_c \gg \lambda$, where r_c is the local radius of curvature of the surface. However, for small θ_{bs} there is an additional spatial lengthscale present: $\lambda/\theta_{\text{bs}}$. While it is clear that the theory is valid in the regime $r_c \gg \lambda/\theta_{\text{bs}}$, it is not obvious to us that this is the case for $\lambda \ll r_c \lesssim \lambda/\theta_{\text{bs}}$. In particular, it is claimed in Ref. [7] p.29 that $r_c \gg \lambda/\theta_{\text{bs}}$ is a necessary condition for the theory to be valid. [As an aside, we also note that in the regime $r_c \gg \lambda$, $\sigma \ll \lambda$, $\theta_{\text{bs}} \gtrsim 1$, the Beckmann-Spizzichino theory predicts an incorrect distribution of scattered light, as can be seen by comparing with the predictions of the smooth-surface theory referred to above, which is based on solving the Helmholtz equation perturbatively in powers of σ/λ .]

These theoretical uncertainties motivate our recommendations 2 and 3, to measure the beam-tube wall's BRDF and its specular reflectivity plus forward scattering in the limit of small incidence angles.

APPENDIX B: RECIPROCITY RELATION FOR SCATTERING INTO AND OUT OF MAIN BEAM

In this appendix we derive the reciprocity relation (16) that relates the probability $dP/d\Omega_{\text{ms}}$ for an interferometer's mirror to scatter photons out of the main beam and into some direction of interest, to the cross section σ_{ms}

for the same mirror to scatter photons arriving from the same direction back into the main beam.

Since the scattering off a very good mirror is produced by mirror irregularities that leave the light's polarization unchanged, we can ignore polarization effects in our analysis and describe the light by a complex scalar electric field, $\psi_z(\vec{y})e^{ikz}$. Our notation is that of paraxial optics: \vec{y} is a location in the plane $z = \text{constant}$ a distance z from the mirror along the optic axis, and the field $\psi_z(\vec{y})e^{ikz}$ is propagating in the $+z$ direction, away from the mirror ("rightward"). We normalize ψ_z such that $|\psi_z|^2 = dI/dA$ is the light's energy flux (power per unit area).

The interferometer's arm cavity supports normal modes labeled by two integers m and n . We denote the modes' rightward propagating eigenfunctions by $\hat{\psi}_{z,mn}(\vec{y})$; they are orthonormal at every z , and most importantly at the mirror's location $z = 0$:

$$\int \hat{\psi}_{z,mn}^* \hat{\psi}_{z,m'n'} d^2y = \delta_{mm'} \delta_{nn'} . \quad (\text{B1})$$

The interferometer's main beam is excited in the $m = 0$, $n = 0$ mode, and as it propagates rightward from the mirror, its field is

$$\psi_{z,\text{mb}} = \sqrt{I_{\text{mb}}} \hat{\psi}_{z,00} . \quad (\text{B2})$$

The factor $\sqrt{I_{\text{mb}}}$ guarantees that the integral of $|\psi_{z,\text{mb}}|^2$ over the transverse plane is equal to the total power I_{mb} carried by the main beam. At the mirror location $z = 0$, the phase fronts of the normal modes and of the main beam match the shape of the mirror (aside from tiny mirror irregularities which produce the light scattering); as a result, when light reflects off the mirror, its normal-mode fields and its main-beam field get phase conjugated: When traveling toward the mirror, the main-beam field is $\sqrt{I_{\text{mb}}} \hat{\psi}_{z,00}^* e^{-ikz}$; when traveling away from the mirror, it is $\sqrt{I_{\text{mb}}} \hat{\psi}_{z,00} e^{ikz}$.

Now consider what happens when the main-beam field reflects off the mirror, taking account of the mirror's tiny imperfections. The imperfections with surface wavelengths $\lambda_{\perp} \leq (L/R_m)\lambda \simeq 1\text{cm}$ scatter light toward the beam-tube baffles and walls or toward non-mirror objects at the other end of the tube; and imperfections with surface wavelengths larger than this scatter light toward the mirror at the other end of the tube, thereby producing mode-mode mixing. The mirror imperfections scatter main-beam light in these manners by putting onto the reflected field a tiny \vec{y} -dependent phase shift $\varphi(\vec{y})$, so the field leaving the mirror, i.e. at $z = 0$, is

$$\sqrt{I_{\text{mb}}} \hat{\psi}_{0,00}(\vec{y}) e^{i\varphi(\vec{y})} . \quad (\text{B3})$$

By propagating the field (B3) down the beam tube using the standard free-space propagator of paraxial optics, or equivalently by using the theory of Fraunhofer diffraction, we infer that the field scattered to a transverse location \vec{y} in the plane a distance z down the tube is

$$\begin{aligned} & \psi_z(\vec{y})e^{ikz} \\ &= \int \frac{-ik}{2\pi z} e^{ikz} e^{ik(\vec{y}-\vec{y}')^2/2z} \sqrt{I_{\text{mb}}} \hat{\psi}_{0,00}(\vec{y}') e^{i\varphi(\vec{y}')} d^2y'. \end{aligned} \quad (\text{B4})$$

Here the integral is over the transverse location \vec{y}' at $z = 0$, i.e. at the mirror plane. The energy flux scattered through the point (z, \vec{y}) is $|\psi_z(\vec{y})|^2$, and the scattering probability $dP/d\Omega_{\text{ms}}(z, \vec{y})$ is this energy flux, multiplied by z^2 to convert it into a power per unit solid angle, and divided by I_{mb} ; the result is

$$\frac{dP(z, \vec{y})}{d\Omega_{\text{mb}}} = \lambda^{-2} \left| \int e^{ik(\vec{y}-\vec{y}')^2/2z} \hat{\psi}_{0,00}(\vec{y}') e^{i\varphi(\vec{y}')} d^2y' \right|^2, \quad (\text{B5})$$

where we have used $k/2\pi = \lambda^{-1}$.

Next consider what happens when light with an energy flux dI/dA arriving from the point (z, \vec{y}) impinges on the mirror. The incoming field at the mirror ($z = 0$) is

$$\psi_{\text{in}} = \sqrt{dI/dA} e^{ik(\vec{y}-\vec{y}')^2/2z}. \quad (\text{B6})$$

Upon reflecting in the mirror, this light will acquire the phase shift $\varphi(\vec{y}')$ due to the mirror's imperfections, plus an additional phase shift due to the mirror's desired curved shape. To avoid dealing with the desired curved shape (which for normal modes just complex conjugates $\hat{\psi}$ but for the field ψ_{in} adds some inhomogeneous non-complex-conjugating phase), we shall put the phase shift φ onto the light mathematically just before it hits the mirror, and then resolve the resulting light into leftward-propagating normal modes of the optical cavity:

$$\psi_{\text{in}}(\vec{y}') e^{i\varphi(\vec{y}')} = \sum_{m,n} c_{mn} \hat{\psi}_{0,mn}^*(\vec{y}'). \quad (\text{B7})$$

The coefficient c_{00} is the amplitude for the mirror imperfections' phase shift φ to scatter the incoming light into the $m = 0, n = 0$ normal mode, i.e., into the main beam. This coefficient can be evaluated using the orthonormality relation (B1):

$$c_{00} = \int \psi_{\text{in}}(\vec{y}') e^{i\varphi(\vec{y}')} \psi_{0,00}(\vec{y}') d^2y'. \quad (\text{B8})$$

The squared modulus of c_{00} is the power δI_{mb} that the incoming light is putting into the main beam; and this power divided by the incoming energy flux dI/dA is the cross section $\sigma_{\text{ms}}(z, \vec{y})$ for light arriving from (z, \vec{y}) to scatter into the main beam. Combining Eqs. (B8) and (B6), we deduce that this cross section is

$$\begin{aligned} \sigma_{\text{ms}}(z, \vec{y}) &= \frac{|c_{00}|^2}{dI/dA} \\ &= \left| \int e^{ik(\vec{y}-\vec{y}')^2/2z} \hat{\psi}_{0,00}(\vec{y}') e^{i\varphi(\vec{y}')} d^2y' \right|^2. \end{aligned} \quad (\text{B9})$$

By comparing this expression for the cross section $\sigma_{\text{ms}}(z, \vec{y})$ with Eq. (B5) for the scattering probability $dP/d\Omega_{\text{ms}}(z, \vec{y})$, we obtain the reciprocity relation

$$\sigma_{\text{ms}}(z, \vec{y}) = \lambda^2 \frac{dP(z, \vec{y})}{d\Omega_{\text{ms}}}. \quad (\text{B10})$$

The backscatter locations (z, \vec{y}) considered in the body of this paper actually lie in the mirror's Fresnel diffraction region (the mirror radius R_{m} is large compared to $\sqrt{\lambda z}$) and not the Fraunhofer region, which is why we have kept the quadratic terms in the phase factor $k(\vec{y} - \vec{y}')^2/2z$ instead of using only the linear term $-k\vec{y}' \cdot (\vec{y}/z)$. This means that in principle the cross section $\sigma_{\text{ms}}(z, \vec{y})$ and scattering probability $dP(z, \vec{y})/d\Omega_{\text{ms}}$ could depend not only on the (vectorial) scattering direction \vec{y}/z but also on distance z from the mirror. In the body of this report we have tacitly assumed (for lack of any experimental data, and as may well be the case) that the spectrum of the mirror's deformations is sufficiently uniform and isotropic across the mirror that, in both the Fresnel and Fraunhofer regions, $\sigma_{\text{ms}}(z, \vec{y})$ and $dP/d\Omega_{\text{ms}}(z, \vec{y})$ depend only on the scalar scattering angle $\theta = |\vec{y}'|/z$ and not significantly on distance z .

APPENDIX C: SCATTERING NOISE FOR OFF-CENTER MIRRORS

Let $\tilde{h}(f; \rho)$ be the gravity-wave noise spectrum due to light backscattering from either baffles or the tube wall when the mirrors are offset from the center of the beam tube by a distance ρR , where R is the beam-tube radius. In this appendix we show that

$$\tilde{h}(f; \rho) = \sqrt{J_n(\rho)} \tilde{h}(f; 0), \quad (\text{C1})$$

where the factor $J_n(\rho)$ by which the noise power \tilde{h}^2 is increased due to off-centered mirrors is

$$J_n(\rho) = \frac{1}{2\pi} \int_0^{2\pi} \frac{d\phi}{\left[\sqrt{1 - \rho^2 \sin^2 \phi} + \rho \cos \phi \right]^{2-n}}, \quad (\text{C2})$$

and where n is the power that appears in the backscatter probability, $dP(\theta)/d\Omega_{\text{bs}} = \beta\theta^n$. For baffles $n = 0$; for bare pipe wall $n = 0$ in the "pessimistic" case, and $n = 1$ in the "optimistic" case. The noise-amplitude increase factor $\sqrt{J_n(\rho)}$ is shown in Fig. 3.

Our starting point is the fundamental formula (12) for the noise from light that backscatters toward an end mirror from a tiny solid angle $\delta\Omega_{\text{ms}}$. This formula is valid whether or not the mirror is at the center of the beam tube. Adopt spherical polar coordinates (θ, φ) centered on the mirror, so that the axis $\theta = 0$ is parallel to the beam-tube symmetry axis but displaced from it by a distance ρR , and so that the beam-tube symmetry axis is in the direction $\varphi = 0$ when $\rho \neq 0$. Then the distance

from the beam axis $\theta = 0$ to the wall of the beam tube in the direction φ is $RG(\varphi)$ where

$$G(\varphi) = \left[\sqrt{1 - \rho^2 \sin^2 \varphi} + \rho \cos \varphi \right]. \quad (\text{C3})$$

In the formula (12), the quantities $dP/d\Omega_{\text{ms}}$, $dP/d\Omega_{\text{bs}}$ and $\tilde{S}^2(f; \theta)$ depend only on θ and not on φ . The only quantity that depends on φ is the distance r from the mirror to the backscattering point, which is given by

$$r = r(\theta, \varphi; \rho) = \frac{RG(\varphi)}{\theta}. \quad (\text{C4})$$

[In the case of baffle backscatter, we ignore small corrections of order (baffle height)/(tube radius) ~ 0.1].

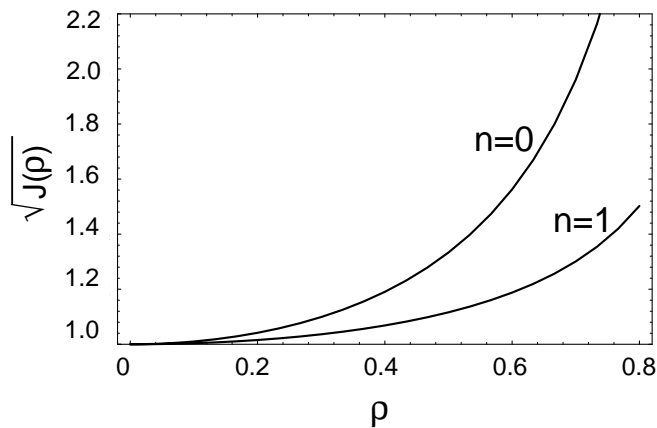


FIG. 3. The factor $\sqrt{J_n(\rho)}$ by which the noise amplitude is increased when the mirrors are offset from the beam-tube center by a distance ρR (where R is the beam-tube radius). The curve $n = 0$ applies to baffles and to the bare beam-tube wall in the “pessimistic” case $dP/d\Omega_{\text{bs}} = \text{constant}$; $n = 1$ is for the bare wall in the “optimistic” case $dP/d\Omega_{\text{bs}} \propto \theta$.

Upon integrating Eq. (12) over solid angle we find that the total noise spectrum takes the form

$$\tilde{h}^2(f; \rho) = \int \int_{\mathcal{D}(\rho)} d\theta d\varphi H(\theta) \frac{1}{r^2(\theta, \varphi; \rho)}, \quad (\text{C5})$$

where $\mathcal{D}(\rho)$ is the domain of integration and $H(\theta)$ is some function which is independent of ρ and φ . Suppose that the domain of integration corresponds to backscattering from distances z down the beam tube in the range $z_2 \leq z \leq z_1$. Let $\theta_1 = R/z_1$, $\theta_2 = R/z_2$. Then the domain of solid angle $\mathcal{D}(\rho)$ of integration for off-centered mirrors is $0 \leq \varphi \leq 2\pi$ and, for each φ , $\theta_1 G(\varphi) \leq \theta \leq \theta_2 G(\varphi)$. By combining Eqs. (C4) and (C5) we obtain

$$\tilde{h}^2(f; \rho) = \frac{1}{R^2} \int_0^{2\pi} d\varphi \frac{1}{G(\varphi)^2} \int_{\theta_1 G(\varphi)}^{\theta_2 G(\varphi)} H(\theta) \theta^2 d\theta. \quad (\text{C6})$$

The function $H(\theta)$ acquires its θ dependence from the solid-angle integration element (one factor of θ), and

from the scattering probabilities ($(dP/d\Omega_{\text{ms}})^2 \propto \theta^{-4}$ and $dP/d\Omega_{\text{bs}} \propto \theta^n$):

$$H(\theta) = H_0/\theta^{3-n}. \quad (\text{C7})$$

Equations (C1) and (C2) can now be obtained by inserting Eq. (C7) into Eq. (C6).

-
- [1] Kip S. Thorne, “Light Scattering and Proposed Baffle Configuration for the LIGO,” LIGO Technical Report, and Caltech Theoretical Astrophysics Preprint number GRP-200 (February 1989), with corrections spelled out in viewgraphs presented to the Sessler Panel, which reviewed LIGO in June 1993. The source of the corrections was Thorne’s omission of a factor B^2 in Eq. (3.5) of GRP-200 — an omission pointed out by Jean-Yves Vinet of the VIRGO Project.
 - [2] Alan W. Greynolds and Gary L. Peterson, “Scatter Analysis of the Basic LIGO Configuration,” Breault Research Organization, Inc. Report #2040 (August 28, 1992); and associated unpublished calculations by Stan Whitcomb and Rainer Weiss (Caltech and MIT, 1992).
 - [3] R. Weiss, “Basis of the Optical Wavefront Specifications,” draft of a LIGO report (March 3, 1994).
 - [4] Gary L. Peterson, “Summary of BRDF and RMS Roughness Measurements Made on Three Steel Samples,” Breault Research Organization, Inc. Report #2190 (January 27, 1993).
 - [5] W. Johnson, D. Stevenson, and K. Clevenger, “Preliminary Seismic Survey of the Livingston LIGO Site,” October 22, 1988 report to the LIGO Project; F. Asiri, verbal description of old underground measurements at the Hanford site.
 - [6] J. M. Elson, H. E. Bennett, and J. M. Bennett, “Scattering from Optical Surfaces,” in *Applied Optical Engineering*, Vol. VII (Academic Press 1979), Chapter 7, pp. 191–243; see especially pp. 223–224.
 - [7] P. Beckmann and A. Spizzichino, *The Scattering of Electromagnetic Waves from Rough Surfaces* (Macmillan/Pergaman, New York, 1963).
 - [8] S. Whitcomb and R. Weiss, private communication.
 - [9] R. Weiss, private communication.
 - [10] R. Weiss, “Optical Properties of the LIGO Beam Tubes”, LIGO memo, January 1989.